Novel Electrochemiluminescence of Silver Nanoclusters Fabricated on Triplex DNA Scaffolds for Label-Free Detection of Biothiols

Lingyan Feng, Li Wu, Feifei Xing, Lianzhe Hu, Jinsong Ren, Xiaogang Qu

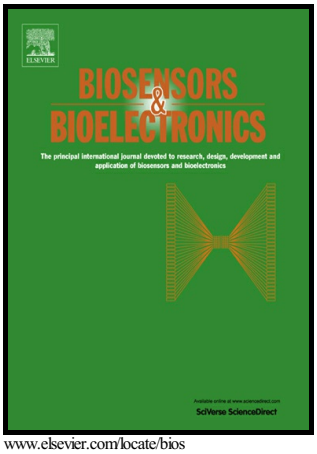

www.elsevier.com/locate/bios

PII: S0956-5663(17)30462-1
DOI: http://dx.doi.org/10.1016/j.bios.2017.07.016
Reference: BIOS9849

To appear in: *Biosensors and Bioelectronic*

Received date: 13 April 2017
Revised date: 21 June 2017
Accepted date: 5 July 2017

Cite this article as: Lingyan Feng, Li Wu, Feifei Xing, Lianzhe Hu, Jinsong Re and Xiaogang Qu, Novel Electrochemiluminescence of Silver Nanocluster Fabricated on Triplex DNA Scaffolds for Label-Free Detection of Biothiols *Biosensors and Bioelectronic,* http://dx.doi.org/10.1016/j.bios.2017.07.016

Novel Electrochemiluminescence of Silver Nanoclusters Fabricated on Triplex DNA Scaffolds for Label-Free Detection of Biothiols

Lingyan Feng[a,*], Li Wu[b], Feifei Xing[c], Lianzhe Hu[d], Jinsong Ren[b], Xiaogang Qu[b,*]

[a]Materials Genome Institute, Shanghai University, 200444 Shanghai, China

[b]Laboratory of Chemical Biology, Division of Biological Inorganic Chemistry, State Key Laboratory of Rare Earth Resource Utilization, Changchun Institute of Applied Chemistry, Chinese Academy of Sciences, 130022 Changchun, China

[c]Department of Chemistry, College of Science, Shanghai University, 200444 Shanghai, China

[d]Chongqing Key Laboratory of Green Synthesis and Applications, and Chongqing Key Laboratory of Inorganic Functional Materials, College of Chemistry, Chongqing Normal University, Chongqing 401331, China

lingyanfeng@t.shu.edu.cn

xqu@ciac.ac.cn

[*]Corresponding author: Tel: +86 021 66136189.

ABSTRACT

Electrochemiluminescence (ECL) of metal nanoclusters and their application have been widely reported due to the good biocompatibility, fascinating electrocatalytic activity and so on. Using DNA as synthesis template opens new opportunities to modulate the physical properties of AgNCs. Triplex DNA has been reported for the site-specific, homogeneous and highly stable silver nanoclusters (AgNCs) fabrication

from our recent research. Here we further explore their extraordinary ECL properties and applications in biosensor utilization. By reasonable design of DNA sequence, AgNCs were obtained in the predefined position of CG.C^+ sites of triplex DNA, and the ECL emission at a low potential was observed with this novel DNA template. Finally, a simple and label-free method was developed for biothiols detection based on the enhanced catalytic reaction and a robust interaction between the triplex-AgNCs and cysteine, by influencing the microenvironment provided by DNA template.

Keywords

silver nanoclusters, electrochemiluminescence, triplex DNA, electrochemical biosensor, biothiols detection

1. Introduction

Noble-metal nanoclusters consisting of several atoms have been gaining much attention owing to their optical/electrochemical properties, which include size-dependent emission wavelength and discrete electronic state, features that are similar to semiconductor quantum dots (Diez et al., 2009; Lee et al., 2005; Tanaka et al., 2011; Yuan et al., 2011; Yu et al., 2007). They have become promising candidates in the fields of cellular imaging and chemical/biological detection owing to their ultrasmall size (< 2 nm), excellent photostability, good biocompatibility and water solubility (Yu et al., 2007; Samanta et al., 2012; Choi et al., 2012). In comparison to the photoluminescence technique, electrogenerated chemiluminescence (ECL) is a light emission that arises from the high-energy electron transfer reaction between

electrogenerated species, which has special advantages such as low cost, wide range of analytes, and high sensitivity (Jie et al., 2008; Hu et al., 2009; Zhan et al., 2007; Miao, 2008). Previous works suggested that metal nanoclusters could be promising materials in ECL investigations. For example, bovine serum albumin (BSA)-stabilized Au nanoclusters (AuNCs) were observed to show high ECL intensity using triethylamine or potassium persulfate as the coreactants commonly used in ECL systems (Li et al., 2011; Fang et al., 2011). As far the silver nanoclusters (AgNCs), individual spatially isolated and bright Ag_2–Ag_8 nanoclusters electroluminescence has been harnessed to create single molecule light-emitting diodes (LEDs) and optoelectronic logic operations (Lee et al., 2005; Vosch et al., 2007; Lee et al., 2003; Lee et al., 2002). Poly-(methacrylic acid) (PMAA) stabilized AgNCs has been reported regarding the hot-electron induced cathodic ECL behavior, however the ECL is only observed under strong cathodic polarization (a pulse voltage of -30 V), which can evoke some unpredictable reactions and thus restrict its development (Diez et al., 2009). Furthermore, the relatively poor stability of AgNCs makes them less desirable in ECL applications (Sharma et al., 2010).

Much effort has been dedicated to synthesize fluorescent AgNCs by using DNA as a template (Petty et al., 2004; Richards et al., 2008; Yeh et al., 2010; Gwinn et al., 2008; Becerril et al., 2009). It has been demonstrated that the properties of AgNCs are highly dependent on the nature of the template molecules used for nanocluster synthesis: the formation of AgNCs relies on the base composition of the DNA template; the stabilities and fluorescence properties of AgNCs are dependent on the

microenvironments provided by DNA templates (Sengupta et al., 2008; Huang et al., 2011a; Huang et al., 2011b). Therefore, the fact that the properties of AgNCs are highly dependent on the nature of the DNA template opens the opportunities to modulate the physical properties of AgNCs by choosing some appropriate DNA templates. While great progress in the ECL performance of DNA-template AgNCs has been recently achieved (Chen et al., 2016; Jie et al., 2017), duplex templates with cytosine/guanine-rich loops were adopted as binding regions for in situ AgNCs formation and ECL achievement. However, there is still room for further improvement, in particular with respect to resolving their stability and homogenous questions, which are quite attractive and challenging for AgNCs fabrication and biosensor applications.

Most recently, a new strategy to create site-specific, homogeneous, and bright AgNCs with high-stability was demonstrated by us using triplex DNA as template (Feng et al., 2012). Triplex has become one of the most useful recognition motifs in the design of new molecular biology tools, diagnostic/therapeutic agents, and construction of DNA-based nanostructures (Chen et al., 2004; Tumpane et al, 2007; Htun et al., 1989). It usually forms through an oligopyrimidine strand binding to the major groove of the duplex parallel to the strand carrying the purine tract using Hoogsteen or reverse Hoogsteen base paring (Becerril et al., 2009; Plum et al., 1990; Song et al., 2005; Feng et al., 2009; Xing et al., 2005; Song et al., 2011). By reasonable design of DNA sequence, homogeneous AgNCs was firstly obtained in the predefined position of CG.C^+ site of triplex DNA (Feng et al., 2012; Ihara et al., 2009). The homogeneity

and ultra-stability against salt of triplex-AgNCs implied that, compared with other AgNCs templates/stabilizer, triplex is more attractive which could provide better protection for the AgNCs against further growth to larger nanostructures and quenching in solution (Feng et al., 2012).

Here we report that the as-prepared triplex-templated AgNCs demonstrated strong ECL emission under much lower potential using sodium persulfate ($Na_2S_2O_8$) as the coreactant. The influence of relative position of $CG.C^+$ triplets and the possible ECL mechanism were discussed according to the presented results, and label-free detection of biothiols was further developed based on the catalytic reaction and microenvironment changes of AgNCs induced by target (Li et al., 2010; Niu et al., 2011; Huang et al., 2011). It indicated that triplex-templated AgNCs could be an effective candidate for new types of ECL biosensors in the future due to their fascinating features, such as ease of labeling and excellent stability.

2. Experimental Section

2.1. Reagents

Silver nitrate ($AgNO_3$, 99.9995%), sodium borohydride ($NaBH_4$, 98%), L-cysteine (98%), and sodium persulfate ($Na_2S_2O_8$, ≥98%) were purchased from Alfa Aesar and used without further purification. All other chemicals were purchased from Sigma-Aldrich and used as supplied. DNA oligonucleotides were purchased from Sangon (Shanghai, China). Phosphate buffer (10mM, 100mM $NaNO_3$, pH=7.2) was used for all the DNA-AgNCs synthesis and fluorescent analysis except that

NH_4Ac/HAc buffer (pH=6.5) was used for MS measurement. Phosphate buffer (10mM, 100mM $Na_2S_2O_8$) was used for all the electrochemical measurements. Nanopure water (18.2MΩ; Millpore Co., USA) was used in all experiments.

2.2 Measurements

Electrochemical measurements were performed in a conventional three-electrode cell (volume of 0.5 mL) with a CH Instruments Model 660B (CHI, Inc.), using an Ag/ AgCl reference electrode (saturated KCl) and a platinum wire counter electrode. ECL intensities were monitored through the bottom of three-electrode cell with a BPCL Ultra-Weak luminescence analyzer, which was purchased from Institute of Biophysics, Chinese Academy of Sciences. Unless otherwise noted, the PMT was biased at 800 V. ECL spectrum was obtained by a series of optical filters (400, 412, 425, 440, 460, 475, 490, 505, 520, 535, 555, 575, 590, 605, 620nm).

Fluorescence spectra were acquired using a Jasco FP-6500 spectrofluorometer (Jasco International Co., Japan). All fluorescence measurements were carried out under ambient temperature using a quartz cell of 1 cm path length. Circular dichroism (CD) spectra were measured on a Jasco J-810 spectropolarimeter with a computer-controlled water bath. The optical chamber of CD spectrometer was deoxygenated with dry purified nitrogen (99.99%) for 45min before use and kept the nitrogen atmosphere during experiments. Three scans were accumulated and automatically averaged.

All the mass spectra were collected on a Thermo LTQ XL ion trap mass spectrometer (Thermo, San Jose, CA, USA) in negative-ion mode. The sample solutions were

infused into the mass spectrometer via a Harvard syringe pump (Holliston, MA, USA) at a flow rate of 5mL/min. The spectra presented represent the average of 200 scans. The needle voltage was set to 3.5k V. The capillary voltage was set to -20V and the tube lens offset to -190V. The heated capillary temperature was set at 250℃ and nitrogen sheath and auxiliary gas flows of 45 and 5 arbitrary units.

2.3. Preparation of fluorescent AgNCs with triplex DNAs as templates

Triplex DNAs were prepared by mixing equimolar amounts of appropriate strands in phosphate buffer, heating to 90℃ and slowly cooling to room temperature. The silver nanoclusters were synthesized by cooling the DNA solution and $AgNO_3$ to 0℃ and then adding $NaBH_4$ followed by vigorous shaking for 2min. The solutions were kept in the dark prior to measurements. Unless otherwise specified, final concentrations were 5 μM for each triplex DNA template, 30μM for $AgNO_3$, and 120μM for $NaBH_4$. The triplex strands for MS spectra are 10μM.

2.4. Immobilization of DNA-AgNCs on electrode surface

Prior to each electrochemical experiment, the glassy carbon electrodes (GCE, Φ=3 mm, CHI) were polished successively with 1.0, 0.3, and 0.05 μm alumina (Buhler) and sonicated for 3min then rinsed thoroughly with water before modification. All experiments were performed at room temperature. 20 μL of each DNA-AgNCs solution was dropped on the GCE surface for following measurements. All the electrodes were thoroughly rinsed with buffer three times.

3. Results and discussion

3.1 ECL properties of triplex-templated AgNCs

The AgNCs using 21mer-triplex T1 DNA (sequence seen supporting information) as template was firstly synthesized as shown in the experimental section following our previous work, named as T1-AgNCs (Feng et al., 2012). TEM image of T1-AgNCs was shown in Figure 1A, with an average diameter calculated about 1.08±0.02 nm (Figure 1B). Here the ECL of T1-AgNCs was directly investigated on glassy carbon electrode (GCE), where the potential was cycled between 0 and -2 V vs. Ag/AgCl (3M KCl) in 10mM phosphate electrolyte buffer containing 100mM $Na_2S_2O_8$, a coreactant commonly used in ECL systems (Figure 1C). We began to observe the ECL signal at the potential of -0.54V, and strong ECL peak for T1-AgNCs constructed electrode located at -1.91V. On the contrary, if using only corresponding duplex (D1) or single strand (ssDNA, S1) as AgNCs templates, both of the presented ECL signals were much weaker (Figure 1C). Such ECL intensities were consistent with their FL results (Figure 1C inset). A strong emission was observed for the T1-AgNCs solution, while comparable weak fluorescence were observed when D1 and S1 used as templates. As the DNA duplex does not act as template for AgNCs, but for Ag nanoparticle (AgNPs) formation (Huang et al., 2011), no obvious enhanced ECL signal was observed in the present of D1-AgNPs complex, suggesting the nanoparticle material was not ECL active. Moreover, only T1 DNA was also not luminescent species for ECL measurement, since its intensity was identical to the background GCE signal (Figure S1). The obtained ECL phenomenon of T1-AgNCs was also consistent with the result recently reported with C-rich looped duplex as

template (Chen et al., 2016).

The obtained ECL intensity of T1-AgNCs solution was quite stable even after incubation with high salt solution (1.5M $NaNO_3$), suggesting that the strong interaction of AgNCs anchored on triplex DNA which ruled out the electrostatic interaction (Figure S2). Our previous work well proved the site-specific AgNCs formation in the $CG.C^+$ triplet through in situ reduction of Ag(I) ions (Feng et al., 2012). The as-prepared T1-AgNCs was stable because of better protection provided by triplex DNA for AgNCs against further growth to larger nanostructures or quenching in solution. No obvious change was observed under consecutive potential scans from 0 to -2V as shown in Figure 1D and Figure S2, which indicated the stable ECL emission of the constructed electrode for further applications.

3.2 Electrochemical characterizations of AgNCs

Electrochemical impedance spectroscopy (EIS) is highly suitable for measuring electrodes surface changes; it allows complex biorecognition events to be probed in a simple, sensitive and mediator-free strategy for rapid analysis (Wu et al., 2012; Feng et al., 2012). The T1-AgNCs composite showed lower electron-transfer resistance (R_{et}) value than that of triplex DNA alone, due to the minor increased conductive property of AgNCs complexes to facilitate electron transfer on surface as shown in Figure 1E (Sharma et al., 2012). Cyclic voltammograms (CV) in Figure S3A show a single anodic process corresponding to the metal-based oxidation of AgNCs (i.e., Ag_n / Ag_n^+ + e^-) with the oxidation peak potential (E_p) at +0.35V vs. Ag/AgCl. It is a surface-controlled progress according to the linear relationship between the peak

current and scan rate (Figure S3B) (Li et al., 2006). The slight shifted positive value of E_p elucidates the high stability of the reduced fluorescent T1-AgNCs species (Sharma et al., 2012). Furthermore, we measured the ECL spectra by employing a series of optical filters, and a distinguished ECL peak located at about 550nm was observed for T1-AgNCs, which was about 20nm red-shift compared to the FL peak (Figure 1F). The phenomenon of red shift can be explained by higher T1-AgNCs concentration used in the ECL measurements than FL experiments, also possible internal filter effects (self-absorption) and instrument effects (Chen et al., 2016; Nepomnyashchii et al., 2013; Swanick et al., 2015; Rashidnadimi et al., 2008).

3.3 Sequence-dependent mass spectra and ECL intensities

In order to demonstrate more evidence for ECL emission of triplex-AgNCs, a series of 14-mer triplex DNA, named as T1C, T2C and T3C, containing same number of $CG.C^+$ and TA.T triplets but different sequences were used for synthesis and characterization of ECL properties (DNA sequences seen Table 1). MS results have proved the presence of Ag atom, Ag_2 clusters and Ag_3 clusters as dominant species in T1C (with discrete $CG.C^+$ triplet site), T2C (with two successive $CG.C^+$ triplet sites) and T3C (with three successive $CG.C^+$ triplet sites), respectively; it further demonstrated the *in situ* reduction of bound Ag (I) ion and the formation of AgNCs in the very position of $CG.C^+$ triplet site in triplex DNA (Figure 2). The Ag atom increased obviously with the increase of $CG.C^+$ numbers, then in situ formed AgNCs on different triplex tempaltes (Feng et al., 2012). By measuring their corresponding ECL spectra, it can be seen that T3C-AgNCs produced strong electroluminescent

which intensity was much higher than those of T2C-AgNCs and T1C-Ag composite as shown in Figure 3A. Distinguished ECL peak at about 543nm was observed for T3C-AgNCs by employing a series of optical filters as shown in Figure 3B, ascribing to the ECL emission of Ag_2 and Ag_3 nanoclusters on triplex. ECL spectrum of these three complexes were consistent with their corresponding photoluminescence spectrum (Figure 3B).

3.4 Triplex-AgNCs ECL mechanism

Few-atom Ag_n nanocluster showed strong ECL emission, which was identical with the inherent electroluminescent readout of single Ag_n(n=2-8) nanoclusters reported (Lee et al., 2002). The photophysical properties of metal nannoclusters differ in character and are controlled by quantum confinement that results in discrete energy levels (Diez et al., 2009). Previous reported cathodic hot electron-induced ECL mechanism of PMMA-stabilized AgNCs was realized on a conductor/insulator/electrolyte surface, in which the insulating layer of metal oxide prevents electron transfer from the metal to a solution species until a large electric field (-30V) exists across the oxide and the Fermi level in the metal is above that of the conduction band of the metal oxide. The current flow across the oxide film can then produce a hot solution-phase electron (Diez et al., 2009; Miao, 2008; Hu et al., 2010; Richter, 2004). Different from previous work, here, the ECL emission of AgNCs was successfully observed under much a lower potential (lower than -2V vs. Ag/AgCl) with the ECL coreactant $Na_2S_2O_8$, making it easier to react. According to the reports about the cathodic ECL of metal nanoclusters and quantum dots (QDs) (Chen et al., 2016; Jie et al., 2008; Li et

al., 2011; Qian et al., 2010), it could be confirmed that the cathodic ECL of Triplex-AgNCs herein was originated from the formation of excited-state AgNCs (Ag_n*) via electron-transfer (ET) annihilation of negatively charged Ag_n $\bullet^-$ and the strongly oxidizing SO4$\bullet^-$ radicals produced by electroreduction of $S_2O_8^{2-}$ (**Scheme 1**). As shown in Figure 4A, the large reduction peak at -0.54 V was attributed to the reduction of $S_2O_8^{2-}$ to anion sulfate radical SO4$\bullet^-$ (Qian et al., 2010). The product, SO4$\bullet^-$, was then reacted with Ag_n $\bullet^-$ by injecting a hole into the highest occupied molecular orbital (HOMO) of Ag_n $\bullet^-$ to obtain an excited state (Ag_n *). This state emitted light in the aqueous solution to produce an ECL signal. The possible ECL mechanisms are described in Scheme 1 with the following equations:

$Ag_n + e^- \rightarrow Ag_n \cdot^-$

$S_2O_8^{2-} + e^- \rightarrow SO_4 \cdot^- + SO_4^{2-}$

$Ag_n \cdot^- + SO_4 \cdot^- \rightarrow Ag_n^* + SO_4^{2-}$

$Ag_n^* \rightarrow Ag_n + h\nu$

3.5 Biothiols detection sensitivity

Biothiols, such as cysteine (Cys), homocysteine (Hcy) and glutathione (GSH), participate important process of many biological redox reaction and monitoring of them is of great importance for disease diagnosis and cellular functions, such as cancer and cardiovascular (Huang et al., 2011). Thus, the development of a simple, lable-free and highly selective method for the detection of biothiols is obviously of significance. L-cysteine (Cys) was chosen for detailed detection as a model thiol compound. Cys has been reported to greatly enhance the ECL intensity of system with

$K_2S_2O_8$ as the coreactant (Niu et al., 2011). It could be easily oxidized to generate RS• radicals, then RS• radicals participate into the reaction of $S_2O_8^{2-}$ to $SO4^{\bullet-}$ radicals (Li et al., 2010; Harman et al., 1984). Under low Cys concentration presented, the above-motioned reaction recycles at the surface of electrode, which gives obvious positive shift of the reduction peak potential of $S_2O_8^{2-}$ from -0.81V to -0.74V (vs. Ag/AgCl), suggesting the enhanced catalytic effect (Figure 4A) (Niu et al., 2011). The ECL excitation pathway of T1-AgNCs is related to the reaction happened between metal species with co-existing agents in the bulk solution (Diez et al., 2009). The reagent $Ag_n^{\bullet-}$ could capture $SO_4^{\bullet-}$ radicals to give ECL emission, and promote the Cys detection sensitively. The advantage of excellent electrical conductivity and fast charge transfer of Triplex-AgNCs gave rise to the strong ECL signal (Figure 1C), making the electrochemical reaction to happen.

Furthermore, the causation of ECL intensity enhancement was not only ascribed to the catalytic reaction. We subsequently turned to the influence of Cys to T1-AgNCs to reveal the other possible reason. As demonstrated in Figure 4B, the fluorescence intensity of T1-AgNCs was found to be obviously enhanced by addition of Cys. Previous study suggested the reason was ascribe to charge transfer from the ligands to the metal center and the change of microenvironment provided by DNA template (Huang et al., 2011). Our CD measurements revealed that the compact structure of triplex was still formed in the presence of low concentration of Cys, which provided protection for AgNCs (Figure S4). Such signal-on pattern could also been developed one fluorescent sensor for the detection of Cys as shown in Figure S5, and the

detection limit of the fluorescent method was calculated to be 5.38μM at 3σ, which was one order lower than the ECL result.

When Cys was injected into the electrolyte, the cathodic ECL of the T1-AgNCs modified GCE showed an obvious increase as shown in Figure 4C. The ECL counts were linearly with the Cys concentration ranging from 0.5 to 50 μM as shown in Figure 4D with a direct detection limit as low as 0.5μM, which was more sensitive than the fluorescent detection limit obtained above. We also compared the present sensor performance with other methods, as summarized in Table 2. The detection limit is also comparable with other Cys detection limits determined by UV and FL optical sensors, as well as other biosensors using AgNCs as probes. Our present work relies on a novel ECL detection scheme using special triplex DNA as AgNCs template, which is generally thermostable and highly site-specific controllable.

3.6 Detection selectivity

In the same way, the prepared T1-AgNCs also responded sensitively for other biothiols, Hcy and GSH detection. There is no obviously distinguish among them. For an excellent sensor, high selectivity is a matter of necessity. To study the specificity of the ECL detection platform for biothiols with T1-AgNCs, 15 kinds of other amino acids were further measured and compared with the ECL signal of Cys under the same concentration of 100μM. The selectivity was shown in Figure 5, and it can be seen that the ECL intensity exhibited a dramatic increase after the addition of biothiols, whereas no obvious enhancements were induced by other amino acids. The excellent selectivity could be attributed to the enhanced catalytic reaction and the specific and robust interaction between the T1-AgNCs and biothiols to influence the microenvironment provided by DNA template. However, ECL intensity of T1-AgNCs would decrease after further increasing the addition of Cys (Figure S6), because large

amount of RS• radicals might complete with $Ag_n^{\bullet-}$ to react with $SO_4^{\bullet-}$radicals to produce SO_4^{2-} thus decrease the ECL signal (Figure 4A). Moreover, triplex CD spectra were also ruined by high concentration of Cys, which would change the microenvironment of AgNCs (Figure S7). The prepared T1-AgNCs also responded sensitively in 20% diluted serum medium. With the addition of different Cys amounts, the ECL intensity increased obviously (Figure 6A). A linear relationship was obtained with lower target presented, and the detection limit was calculated as 0.71 uM at 3σ (Figure 6B).

Due to the high complexity of the DNA-AgNCs system and the lack of adequate understanding of chemical and spectral properties of DNA-AgNCs, it is still a challenge for us to fully understand the detailed mechanism driving these different ECL response patterns and work is still in progress. In addition, how to further distinguish biothiols separately is also an important issue in future.

4. Conclusion

In conclusion, we have reported the ECL emission from AgNCs using well-designed triplex DNA as template. The ECL behavior and mechanism of site-specific, highly stable triplex-templated AgNCs have been studied in detail and further been used for the signal-on and sensitive detection of biothiols. The reason could be ascribed to cathodic coreactant ECL based on the enhanced catalytic reaction and microenvironment changes of AgNCs influenced by biothiols according to the presented results. This work widely expands the investigation on ECL of metal clusters, and the triplex-templated AgNCs would be promising candidates in the ECL analysis with the advantages of stability and easier preparation.

Acknowledgements

This work is sponsored by Shanghai Sailing Program (No.17YF1405700), the National Natural Science Foundation of China (Grant 21401127, Grant 21605012) and Scientific and Technological Research Program of Chongqing Municipal Education Commission (No. KJ1600301). We also thank the support of the Shanghai Institute of Materials Genome from the Shanghai Municipal Science and Technology Commission, as well as the Program for Professor of Special Appointment (Eastern Scholar) at the Shanghai Institution of Higher Learning (No. TP2016023).

References

Becerril, H.; Woolley, A., 2009, Chem. Soc. Rev., 38, 329-337.

Chen, A.; Ma, S.; Zhuo, Y.; Chai, Y.; Yuan, R., 2016, Anal. Chem., 16, 88, 3203-3210.

Chen, Y.; Lee, S. H.; Mao, C., 2004, Angew. Chem. Int. Ed., 43, 5335-5338.

Chen, Z.; Lu, D.; Cai, Z.; Dong, C.; Shuang, S., 2014, Luminescence, 29, 722-727.

Choi, S.; Dickson, R. M.; Yu, J., 2012, Chem. Soc. Rev., 41, 1867-1891.

Diez, I.; Pusa, M.; Kulmala, S.; Jiang, H.; Walther, A.; Goldmann, A. S.; et al., 2009, Angew. Chem. Int. Ed., 48, 2122-2125.

Ding, Z.; Quinn, B.; Haram, S.; Pell, L.; Korgel, B.; Bard, A., 2002, Science, 296, 1293-1297.

Fang, Y.; Song, J.; Li, J.; Wang, Y.; Yang, H.; Sun, J.; Chen, G., 2011, Chem. Commun. 47, 2369-2371.

Feng, L.; Chen, Y.; Ren, J.; Qu, X., 2011, Biomaterials, 32, 2930-2937.

Feng, L.; Huang, Z.; Ren, J.; Qu, X., 2012, Nucleic Acid Res. e122.

Feng, L.; Li, X.; Peng, Y.; Geng, J.; Ren, J.; Qu, X., 2009, Chem. Phys. Lett., 480, 309-312.

Feng, L.; Wu, L.; Wang, J.; Ren, J.; Miyoshi, D.; Sugimoto, N.; Qu, X., 2012, Adv. Mater., 24, 125-131.

Guo, J.; Kong, D.; Shen, H., 2010, Biosens & Bioelectron., 26, 327-332.

Gwinn, E.; O'Neill, P.; Guerrero, A.; Bouwmeester, D.; Fygenson, D., 2008, Adv. Mater., 20, 279-283.

Harman, L.; Mottley, C.; Mason, R., 1984, J. Bio. Chem., 259, 5606-5611.

Hu, L.; Bian, Z.; Li, H.; Han, S.; Yuan, Y.; Gao, L.; Xu, G., 2009, Anal. Chem. 81, 9807-9811.

Hu, L.; Xu, G., 2010, Chem. Soc. Rev., 39, 3275-3304.

Hu, M.; Fan, J.; Li, H.; Song, K.; Wang, S.; Cheng, G.; Peng, X., 2011, Org. Biomol. Chem., 9, 980-983.

Huang, Z.; Pu, F.; Hu, D.; Wang, C.; Ren, J., Qu, X., 2011a, Chem. Eur. J., 17, 3774-3780.

Huang, Z.; Pu, F.; Lin, Y.; Ren, J., Qu, X., 2011b, Chem. Commun., 47, 3487-3489.

Htun, H.; Dahlberg, J. E., 1989, Science, 243, 1571-1576.

Ihara, T.; Ishii, T.; Araki, N.; Wilson, A. W.; Jyo, A., 2009, J. Am. Chem. Soc., 131, 3826-3827.

Jiang, X.; Zhang, J.; Shao, X.; Zhao, W., 2012, Org. Biomol. Chem., 10, 1966-1968.

Jie, G.; Tan, L.; Zhao, Y.; Wang, X., 2017, Biosens & Bioelectron., 94, 243-249.

Jie, G.; Zhang, J.; Wang, D.; Cheng, C.; Chen, H. Y.; Zhu, J. J., 2008, Anal. Chem., 80, 4033-4039.

Lee, T.; Dickson, R., 2003, Proc. Natl. Acad. Sci. U. S.A. 100, 3043-3046.

Lee, T.; Gonzalez, J.; Dickson, R., 2002, Proc. Natl. Acad. Sci. U. S.A. 99, 10272-10275.

Lee, T.; Gonzalez, J.; Zheng, J.; Dickson, R., 2005, Acc. Chem. Res., 38, 534-541.

Li, T., Shi, L.; Wang, E.; Dong, S., 2009, Chem. Eur. J., 15, 3347-3350.

Li, G.; Yang, J.; Zheng, X.; Meng, M.; Cao, J., 2010, Microchimica Acta, 168, 277-282.

Li, L.; Liu, H.; Shen, Y.; Zhang, J.; Zhu, J. J., 2011, Anal. Chem., 83, 661-665.

Miao W., 2008, Chem. Rev., 108, 2506-2553.

Li, X.; Peng, Y.; Ren, J.; Qu, X., 2006, Biochemistry, 45, 13543-13550.

Nepomnyashchii, A. B.; Pistner, A. J.; Bard, A. J.; Rosenthal, J. 2013, J. Phys. Chem.

C, 117, 5599−5609.

Liu, J.; Sun, Y.; Huo, Y.; Zhang, H.; Wang, L.; Zhang, P.; Song, D.; Shi, Y.; Guo, W., 2014, J. Am. Chem. Soc., 136, 574−577.

Niu, H.; Yuan, R.; Chai, Y.; Mao, L.; Yuan, Y.; Zhuo, Y.; Yuan, S.; Yang, X., 2011, Biosens. Bioelectron., 26, 3175-3180.

Petty, J.; Zheng, J.; Hud, N.; Dickson, R., 2004, J. Am. Chem. Soc., 126, 5207-5212.

Plum, G.; Park, Y.; Singleton, S.; Dervan, P.; Breslauer, K., 1990, Proc. Natl. Acad. Sci. U. S.A. 87, 9436-9440.

Qian, J.; Zhang, C.; Cao, X.; Liu, S., 2010, Anal. Chem., 82, 6422-6429.

Richards, C.; Choi, S.; Hsiang, J.; Antoku, Y.; Vosch, T.; Bongiorno, A.; Tzeng, Y.; Dickson, R., 2008, J. Am. Chem. Soc., 130, 5038-5039.

Samanta, P.; Periyasamy, G.; Manna, A.; Pati, S., 2012, J. Mater. Chem., 6774-6781.

Sengupta, B.; Ritchie, C. M.; Buckman, J. G.; Johnsen, K. R.; Goodwin, P. M.; Petty, J. T., 2008, J. Phys. Chem. C. 112, 18776-19782.

Sharma, J.; Rocha, R. C.; Phipps, M. L.; Yeh, H. C.; Balatsky, K. A.; Vu, D. M.; et al., 2012, Nanoscale, 4, 4107-4110.

Sharma, J.; Yeh, H. C.; Yoo, H.; Werner, J. H.; Martinez, J. S., 2010, Chem. Commun. 46, 3280-3282.

Shiu, H.; Wong, M.; Che, C., 2011, Chem. Commun. 47, 4367-4369.

Song, G.; Xing, F.; Qu, X.; Chaires, J.; Ren, J., 2005, J. Med. Chem., 48, 3471-3473.

Song, Y.; Feng, L.; Ren, J.; Qu, X., 2011, Nucleic Acids Res., 39, 6835-6843.

Sun, J.; Yang, F.; Zhao, D.; Chen, C.; Yang, X., 2015, ACS Appl. Mater. Interfaces, 7, 6860-6866.

Swanick, K. N.; Sandroni, M.; Ding, Z.; Zysman-Colman, E. 2015, Chem. Eur. J., 21, 7435−7440.

Rashidnadimi, S.; Hung, T. H.; Wong, K.-T.; Bard, A. J. 2008, J. Am. Chem. Soc., 130, 634−639.

Richter, M., 2004, Chem. Rev., 104, 3003-3036.

Tanaka, S.; Miyazaki, J.; Tiwari, D.; Jin, T.; Inouye, Y., 2011, Angew. Chem. Int. Ed., 50, 431-435.

Tumpane, J.; Kumar, R.; Lundberg, E. P.; Sandin, P.; Gale, N.; Nandhakumar, I. S.; Albinsson, B.; Lincoln, P,; Wilhelmsson, L. M.; Brown, T.; Norden, B., 2007, Nano

Lett., 7, 3832-3839.

Vosch, T.; Antoku, Y.; Hsiang, J. C.; Richards, C. I.; Gonzalez, J. I.; Dickson, R. M., 2007, Proc. Natl. Acad. Sci. U. S.A. 104, 12616-12621.

Wu, L.; Wang, J.; Feng, L.; Ren, J.; Qu, X., 2012, Adv. Mater., 24, 2447-2452.

Xing, F.; Song, G.; Ren, J.; Chaires, J.; Qu, X., 2005, FEBS Lett., 579, 5035-5039.

Yang, Z.; Zhao, N.; Sun, Y.; Miao, F.; Liu, Y.; Liu, X.; et al., 2012, Chem. Commun., 48, 3442-3444.

Yeh, H.; Sharma, J.; Han, J.; Martinez, J.; Werner, J., 2010, Nano Lett., 10, 3106-3110.

Yu, J.; Patel, S. A.; Dickson, R. M., 2007, Angew. Chem. Int. Ed., 46, 2028-2030.

Yuan, L.; Lin, W.; Yang, Y., 2011, Chem. Commun., 47, 6275-6277.

Yuan, X.; Luo, Z,; Zhang, Q.; Zhang, X.; Zheng, Y.; Lee, J. Y.; Xie, J., 2011, ACS Nano., 5, 8800-8808.

Zhan, W.; Bard, A. J., 2007, Anal. Chem., 79, 459-463.

Zhu, B.; Zhang, X.; Li, Y.; Wang, P.; Zhang, H.; Zhuang, X., 2010, Chem.Commun., 46, 5710–5712.

Figure Captions

Scheme 1: Schematic representation of the binding motif of reduced Ag atom to CG.C^+ triplet and the ECL mechanism of triplex templated AgNCs.

Figure 1: (A) TEM image of 21 mer-T1 templated AgNCs, with scale of 10 nm. (B) The diameter of T1-AgNCs, and the number of cluster counts for histogram was 105, with an average diameter about 1.08±0.02 nm. (C) ECL of T1, D1, S1-Ag composites anchored on electrode surface. DNA concentration is 5μM. inset: fluorescence emission spectra acquired for T1, D1, S1 solutions, upon excitation at 480nm. DNA concentration is 2μM. (D) The stability of ECL of T1, D1, S1-Ag composites. (E) EIS of bare GCE (black), T1/GCE (red), T1-AgNCs/GCE (blue). (F) ECL (blue) and FL

(red) spectrum of the as-prepared T1-AgNCs. DNA concentration is 5μM.

Figure 2: ESI-TOF mass spectra of T1C, T2C and T3C.The ratio of Ag(I) ions to DNA is 1:1, DNA concentration is 10μM.

Figure 3: (A) ECL of T1C, T2C, T3C-Ag composites anchored on electrode surface. DNA concentration is 5μM. (B) the corresponding ECL spectra of T1C, T2C, T3C-Ag composites.

Figure 4: (A) CV of the as-prepared T1-AgNCs after addition of 40, 200, and 500 μM Cys. (B) FL and (C) ECL spectra of T1-AgNCs after addition of different concentrations of Cys from 5μM to 300μM. (D) ECL data of the as-prepared T1-AgNCs after addition of different concentrations of Cys. Inset: the linear relationship between ECL accounts and the concentrations of Cys.

Figure 5: Selectivity of ECL of the as-prepared AgNCs on GCE for biothiols (Cys, Hcy and GSH) detection. All amino acid concentration was 100μM.

Figure 6: The ECL responses of T1-AgNCs with different Cys concentrations in 20% diluted serum medium, (A) Cys concentrations (from a to i): 0, 1, 3, 5, 8, 10, 20, 50 and 80 uM. The solutions were prepared by spiking standard Cys solutions at certain concentration as stock solutions. (B) The relationship between Cys concentration and ECL count points, inset: the linear relationship with lower target presented from from 0 to 10 uM, R^2=0.96.

Scheme 1

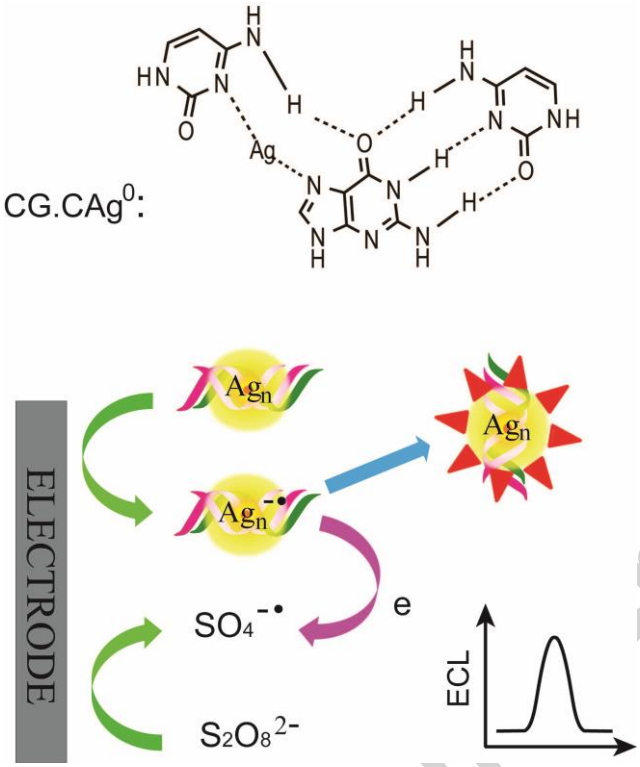

Figure 1

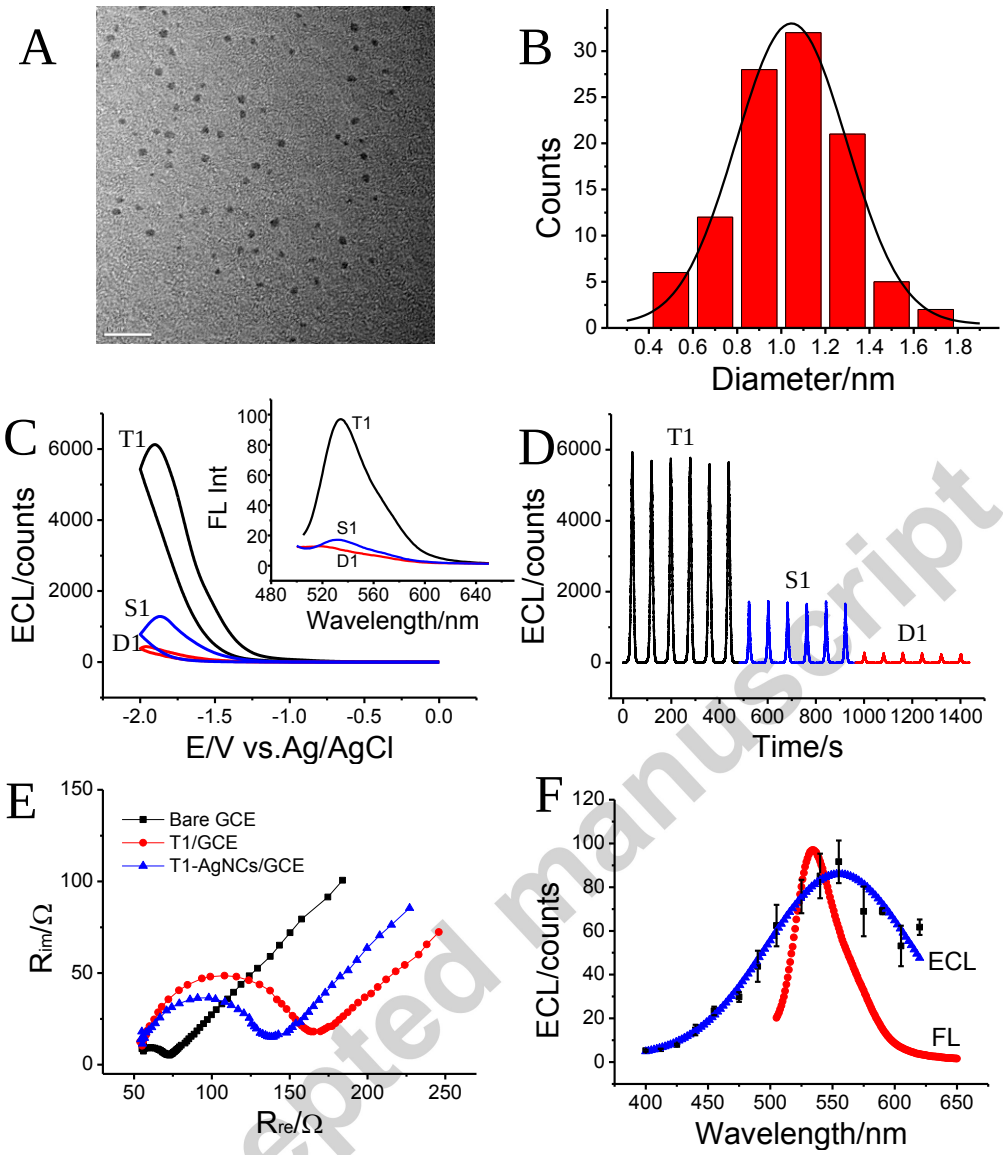

Figure 2

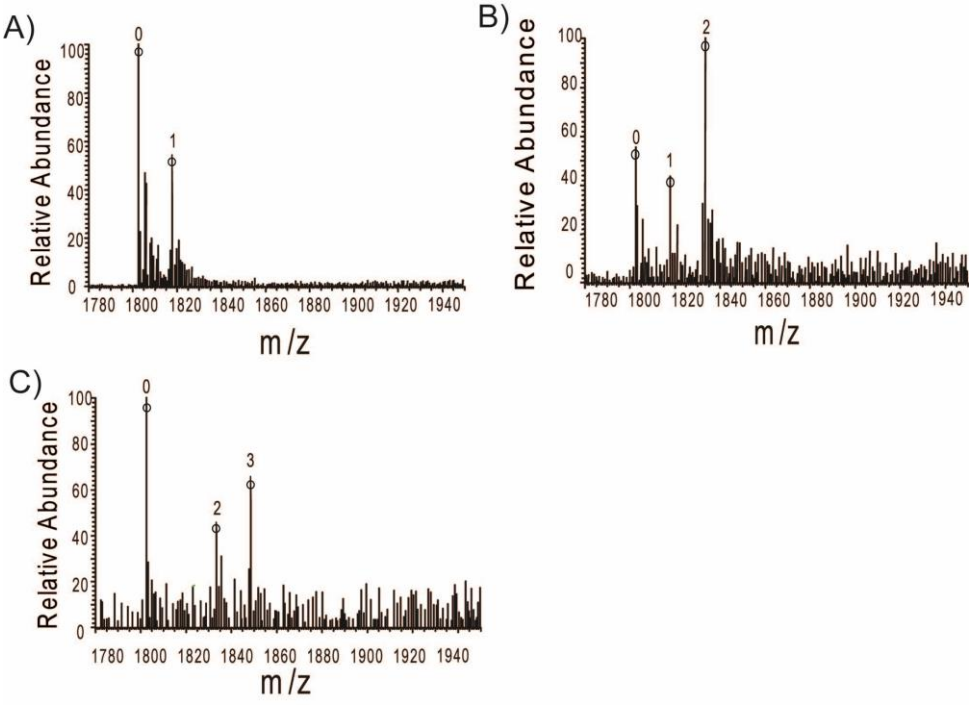

Figure 3

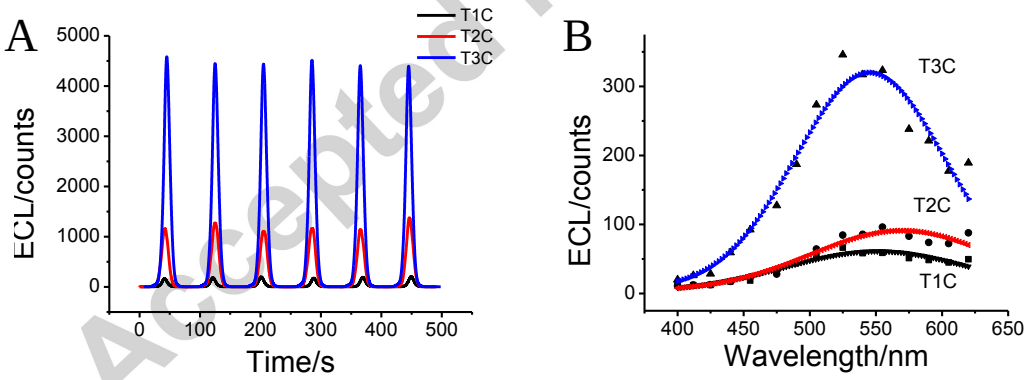

Figure 4

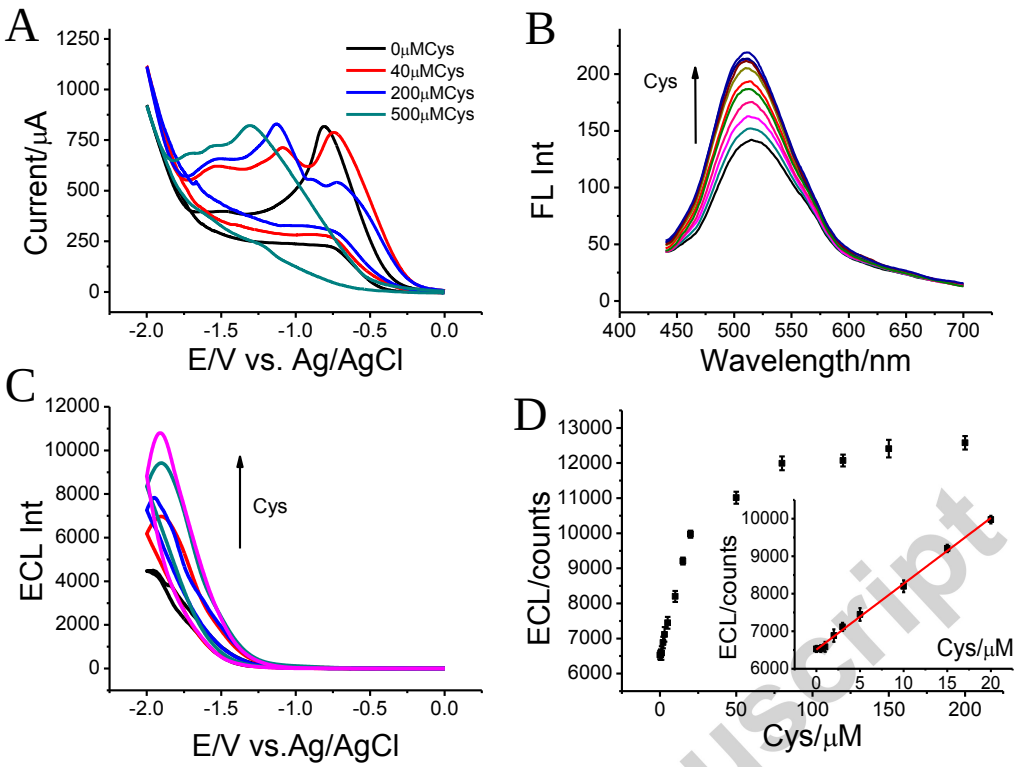

Figure 5

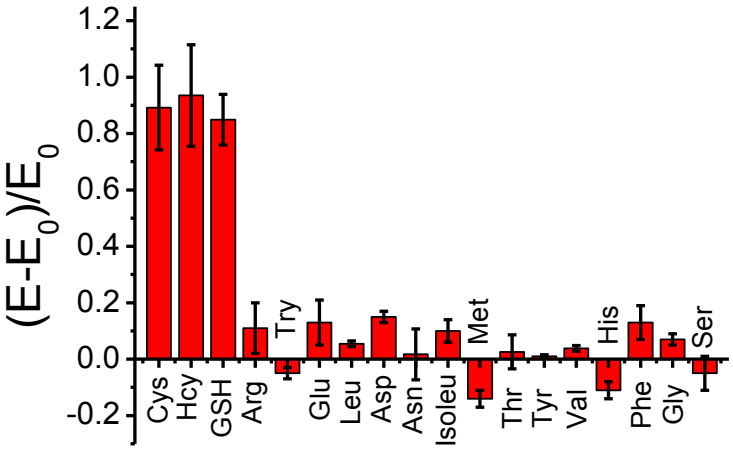

Figure 6

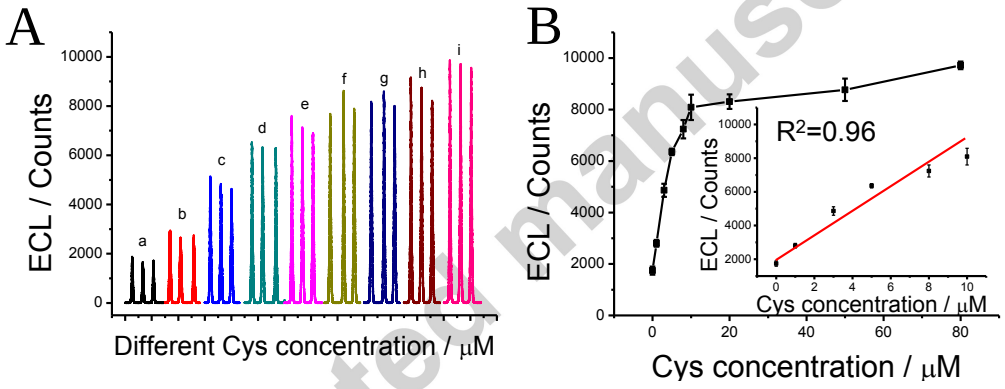

Table 1: The sequences and a labeling scheme of DNA used in this study.

Name	Sequences (5′-3′)	Base length
Triplex 1 (T1)	5′-GAG AGG AGA GAG AAG AGG AAG-3′ 3′- CTC TCC TCT CTC TTC TCC TTC -5′ 5′-CTC TCC TCT CTC TTC TCC TTC-3′	21
Duplex 1 (D1)	5′-GAG AGG AGA GAG AAG AGG AAG-3′ 3′- CTC TCC TCT CTC TTC TCC TTC -5′	21
S1	5′-CTC TCC TCT CTC TTC TCC TTC-3′	21
T1C	5′-TCTCTCTCTCTCTT-3′ 3′-AAGAGAGAGAGAGA-5′ 5′-TTCTCTCTCTCTCT-3′	14
T2C	5′-TTCCTTCCTTCCTT-3′ 3′-AAGGAAGGAAGGAA-5′ 5′-TTCCTTCCTTCCTT-3′	14
T3C	5′-TTCCCTTTTCCCTT-3′ 3′-AAGGGAAAAGGGAA-5′ 5′-TTCCCTTTTCCCTT-3′	14

Table 2: **Comparison of the present work with other reported Cys sensors.**

Different detection methods		**Detection limits**	**References**
UV-Vis absorption methods	Silver ion mediated DNAzyme switch	0.4 μM	Li et al. 2009
	Naphthalimide-based colorimetric probe	28 μM	Zhu et al. 2010
Fluorescent methods	Synthesized fluorescent probe	0.75 μM	Yuan et al. 2011
	Fluorescent chemodosimeter	0.68 μM	Hu et al. 2011
	Chlorinated coumarin-hemicyanine dye	0.05 μM	Liu et al. 2014,
	Two-photo fluorescent probe	293 μM	Yang et al., 2012
	Triphenylemethane dye/G-quadruplex complexes	0.059 μM	Guo et al., 2010
	Fluorescent NIR probe	0.5 μM	Jiang et al. 2012
	Luminescent iridium (III) probe	130 μM	Shiu et al. 2011
Silver nanocluster	BSA-confined AgNCs as fluorometric probe	0.81 μM	Chen et al., 2014
	Ag/Au bimetallic nanocluster	0.11 μM	Sun et al., 2015
Present work, fluorescent method		5.38 μM	
Present work, ECL method		0.5 μM	

Highlights

- Electrochemiluminescence of silver nanoclusters (AgNCs) with triplex DNA as template is reported.
- Reasonable design of triplex sequence to control AgNCs fabrication positions and emission intensities.
- Simple and label-free biothiols detection is developed through the enhanced catalytic reaction and interaction.